

Collisional dynamics of vortices in light condensates

María J. Paz-Alonso, David Olivieri, Humberto Michinel, and José R. Salgueiro

Area de Óptica, Facultade de Ciencias de Ourense, Universidade de Vigo, As Lagoas s/n, Ourense, ES-32004 Spain

(Received 20 December 2003; published 4 May 2004)

Through numerical simulation, we have studied the nucleation and annihilation of two-dimensional optical vortex solitons hosted in finite size light beams. Our study covers a wide range of angular momentum $l \geq 1$, also referred to as its topological charge. We demonstrate that surface tension of light beams prevents beam filamentation for a certain range of total reflection angles even if the hosted hole splits and decays into several vortices with lower values of l . We also discuss a mechanism for vortex nucleation starting from Gaussian beams that can be used for experimental purposes. Our work adds extra support to the idea that light beams in cubic-quintic nonlinear materials can undergo a phase transition from a photon gas to a liquid of light.

DOI: 10.1103/PhysRevE.69.056601

PACS number(s): 42.65.Tg, 42.65.Jx

I. INTRODUCTION

Vortices [1] are present in very different branches of physics such as fluid mechanics, Bose-Einstein condensation, astrophysics and laser dynamics, among others [2]. Optical fields that exhibit phase singularities manifest themselves as isolated dark spots in the modal patterns of certain lasers [3]. Each dark spot has a topological charge l that represents the number of windings of the phase around the singularity [4]. The wave fronts near a singularity have a helical structure, while the field at the singularity must be zero because of the ambiguous phase, hence the dark spot. These defects can be produced by appropriately shining a computer generated hologram [5] or by propagation through turbulent optical media.

Concerning propagation in the nonlinear regime [6], the first theoretical work analyzed their stability in Gaussian-like distributions propagating in optical Kerr materials [7]. It was found that for a cubic self-focusing refractive index, a beam of finite size will always filament under the action of a phase dislocation [8]. This also holds true for saturable self-focusing nonlinearities [9,10]. On the other hand, vortex states were predicted and found experimentally for self-defocussing materials both in the Kerr case for continuous background [11] and in the saturable case with finite size beams [12].

It was also shown in Ref. [13] that stable vortex states with angular momentum $l=1$ can be obtained as stationary states of the propagation of a laser beam through cubic-quintic nonlinear optical materials [14]. The refractive index of this kind of materials has a maximum for a given intensity. The formation of such vortices is achieved when a Gaussian laser beam with power over a critical threshold shines a phase mask.

Previous studies have also elucidated the dynamical properties associated with light condensates with some kind of surface tension properties [15]. In this work it has been shown that laser beams with almost square profiles, which are the eigenstates of the cubic-quintic Schrödinger equation, behave in a similar way as liquids with surface tension properties. More surprisingly, it has been found that the stability of such vortex eigenstates is a natural consequence of the nonlinear Schrödinger equation. In this paper, we explore the

collisional dynamics of such stable vortex eigenstates.

We shall focus our attention in this article upon the effect of surface tension of laser beams with angular momentum. Our interest shall be to demonstrate that surface tension prevents beam filamentation even in the case of total reflections where the inner vortex can split into several holes with different values of l .

After brief introduction of the governing equations, the numerical simulations shall be described. The 2D nonlinear Schrödinger equation (NLSE) is used for simulating the propagation of stable vortex eigenfunctions in cubic-quintic materials. The initial vortex eigenstates have been obtained by integrating the stationary NLSE. Our simulations demonstrate that a relation between surface tension [16] and optical stable azimuthal states exists as a function of the topological quantized charge l .

The structure of this article is as follows. Before presenting our results, we shall briefly describe the physical configuration represented in our model for creating optical vortex eigenstates together with the governing nonlinear Schrödinger equation. While coalescence or nonlinear filtering are candidates for the creation of stable eigenstates, our simulations assume a given vortex eigenstate distribution, obtained from stationary state solutions of the NLSE. We will also analytically calculate the critical values of the propagation constant and peak amplitude that characterize the domain existence of the vortices.

For several vortex eigenstates with different topological charges l and for different number densities ρ , we first establish long term stability to small amplitude perturbations. Next, the results of large amplitude perturbation, in the form of collisions with planar surfaces, are presented. Detailed surface waves have been measured and a condition for vortex breaking is given.

II. PHYSICAL MODEL

The equation for paraxial propagation along z , of a continuous linearly polarized laser beam, in a nonlinear optical material with a intensity-dependent refractive index, is governed by a generalized nonlinear Schrödinger equation (NLSE), given as follows:

$$2ikn_0 \frac{\partial \Psi}{\partial z} + \nabla_{\perp}^2 \Psi + 2k^2 n_0 f(|\Psi|^2) \Psi = 0, \quad (1)$$

where $k=2\pi/\lambda$ is the wave number in vacuum, n_0 is the linear refractive index, $|\Psi|^2$ is the intensity of the electromagnetic wave, and $\nabla_{\perp}^2 = r^{-2} \partial^2 / \partial \theta^2 + r^{-1} \partial / \partial r + \partial^2 / \partial r^2$ is the transverse Laplacian operator in cylindrical coordinates (r, θ, z) . The function $f(|\Psi|^2)$ indicates the dependence of the nonlinear refractive index with the beam power. To achieve the phase transition from a gas state to a liquid light state, f must have a maximum at a given beam intensity. A simple model with this property is the cubic-quintic nonlinearity [17,18], where $f(|\Psi|^2) = n_2 |\Psi|^2 - n_4 |\Psi|^4$, such that the positive constants n_2 and n_4 capture the dependence of the refractive index on the intensity of the beam. Physically, the combined effect of diffraction and the self-defocusing term of n_4 , will balance the collapsing tendency induced by the Kerr effect, giving rise to a stable two-dimensional light distribution [19].

III. STRUCTURE OF VORTEX STATES

We performed the numerical integration of Eq. (1) for stationary vortex states [13] of the form $\Psi(r, \theta, z) = \psi(r) e^{i(\beta z + l\theta)}$, where $r = (x^2 + y^2)^{1/2}$ is the radial dimension, β the nonlinear phase shift or propagation constant, and $\theta = \tan^{-1}(y/x)$. For a given integer value of l , a continuum of eigenstates can be obtained with β varying between zero and a critical value β_{cr} over which no stationary states can be found. In the limit $r \rightarrow \infty$, terms $r^{-1} \partial \Psi^2 / \partial \theta^2$ and $r^{-1} \partial \Psi / \partial r$ tend to zero, so that Eq. (1) yields a one-dimensional equation of the form

$$\frac{\beta}{kn_4} \psi - \frac{1}{2k^2 n_0 n_4} \psi_{rr} - \frac{n_2}{n_4} \psi^3 + \psi^5 = 0. \quad (2)$$

We obtain a solution similar to the one given in Ref. [14]:

$$\psi^2(r) = \frac{3n_2}{4n_4 2a} \frac{1 - a^2}{\cosh^2(k\sqrt{2\beta n_0} r) + 1 - a}, \quad (3)$$

where the dimensionless parameter a is given by $a = \sqrt{1 - 16\beta n_4 / 3kn_2^2}$.

By imposing that the beam power is equal to $N = 2\pi \int_0^{\infty} \psi^2(r) r dr$, we get

$$\beta = \frac{3kn_2^2}{16n_4} \tanh^2(\sqrt{2/3} N). \quad (4)$$

Thus, N is directly related to a by $a = 1 / \cosh(\sqrt{2/3} N)$.

In the limit $N \rightarrow \infty$ a goes to zero, so that we obtain the critical value of the propagation constant β_{cr} and the amplitude A_{cr} : $\beta_{cr} = 3kn_2^2 / 16n_4$ and $|A_{cr}|^2 = 3n_2 / 4n_4$. Note that the previous critical values do not depend on the angular momentum l of the beam.

It can be shown that low values of β yield low values of the beam power N and light distributions with Gaussian-like peaks. As β is increased, the beam flux grows and the spatial shapes tend to narrow, producing a minimum width and a maximum peak intensity of the stationary states, for a given

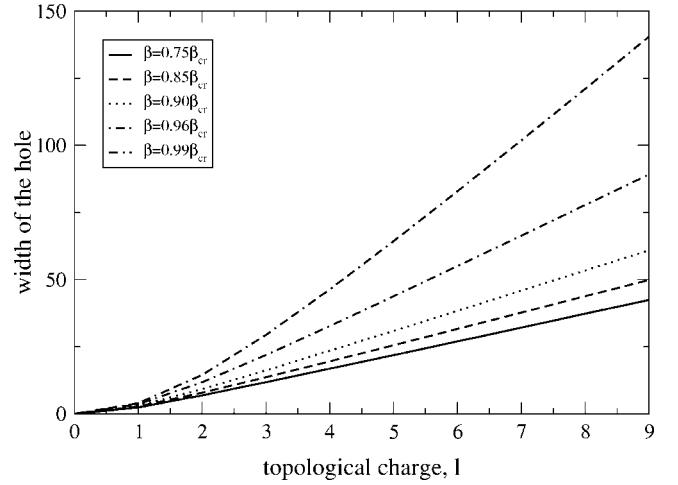


FIG. 1. Dependence of the width of the hole versus topological charge l for different values of the propagation constant β .

power. For larger values of β , the beam flux grows rapidly and the peak intensity of the light distribution saturates due to the effect of n_4 .

For larger powers, the spatial light distributions converge towards wide flat-top profiles with sharp decaying edges [20,21], similar to hyper-Gaussian distributions. We have also detected a slow decrease of $d\psi/dr$ at $r=0$ for large values of N . We must also stress that the limit $\beta \rightarrow 0$ yields to a nonzero value of the beam power.

In this paper we will study laser beams with approximately square profiles, as described previously, for different values of the angular momentum $l > 1$, which are the eigenstates of the cubic-quintic NLSE. As can be seen in Figs. 1 and 2, the central hole of the beam increases its size with the topological charge l , while the size of the corona saturates for high values of the angular momentum. Note that this behavior occurs for any value of the propagation constant β . Close to β_{cr} , the beams are almost square shaped. In this limited case, it is possible to derive an analytical expression

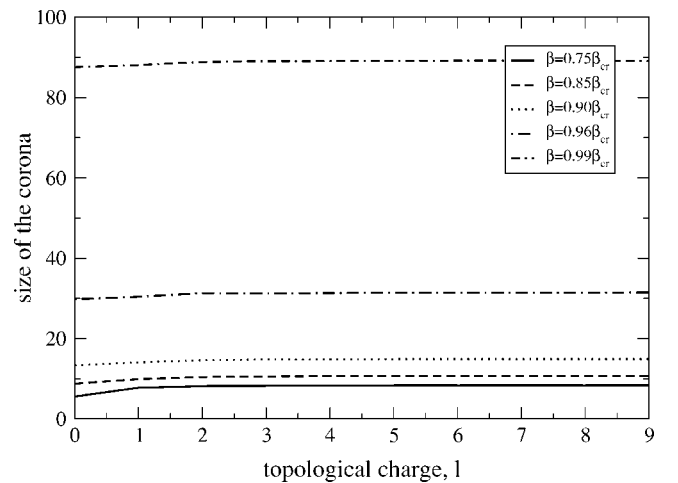


FIG. 2. Dependence of the size of the corona of the vortex versus topological charge l for different values of the propagation constant β .

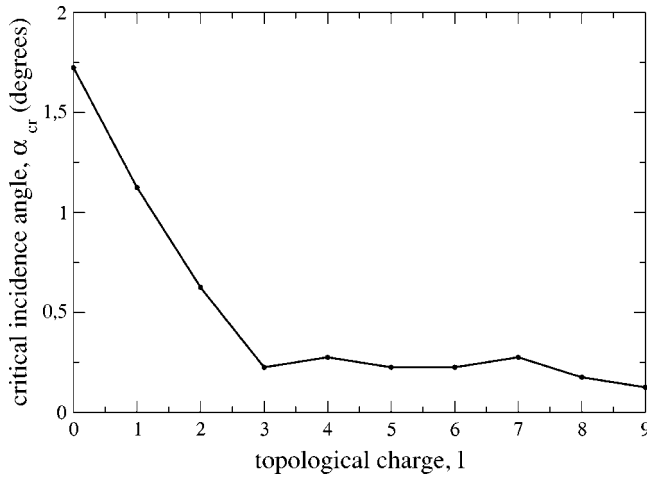


FIG. 3. Dependence of the critical angle of incidence α_{cr} versus topological charge l . The propagation constant is $\beta=0.95\beta_{cr}$.

for the surface tension of these light condensates. To do so, we express the increase of the system energy using the Hamiltonian $dH = [\frac{1}{2}|\nabla\Psi|^2 - \frac{1}{2}(n_2/n_4)|\Psi|^4 + \frac{1}{3}|\Psi|^6]2\pi r dr$, and we consider a thermodynamical model with $dH = \mu dN - \sigma dA$. By analogy with Bose-Einstein condensates in alkali gas, β plays the role of a chemical potential μ . Thus, σdA represents the work due to deformation against a surface tension σ . Considering a square eigenstate function of radius r , we obtain

$$\sigma = \frac{9\pi}{16} \left(\frac{n_2}{n_4} \right)^3 r. \quad (5)$$

Thus, the surface tension of the light condensates grows linearly with the radius, as in the case of usual liquid droplets. This adds extra support to the idea that light beams in cubic-quintic nonlinear materials can undergo a phase transition from a photon gas to a liquid of light.

IV. NUMERICAL SIMULATIONS OF PROPAGATION

In order to test the stability of the vortex states that we have previously described, we present in this section results for the propagation of beams with a nested vortex through a bulk cubic-quintic nonlinear optical material in the presence of a planar boundary. The propagation equation for the above waveguide in the paraxial regime is a generalized NLSE, including the effect of boundaries. The input beam impacts the boundary with a given incidence angle α (initial velocity of the equivalent particle) and suffers a total reflection. For low values of the initial velocity, the collision is quasielastic. This means that the emerging beam will preserve a compact support with the nested vortex. Above a critical value of the incidence angle α_{cr} which depends upon the value of l , the vortex is annihilated and the compact support may produce several filaments, depending upon the initial conditions.

In Fig. 3 we show the dependence of the critical incidence angle α_{cr} versus the topological charge l for a propagation constant $\beta=0.95\beta_{cr}$. As can be appreciated, there is a fast decrease of the critical incidence angle for low values of the

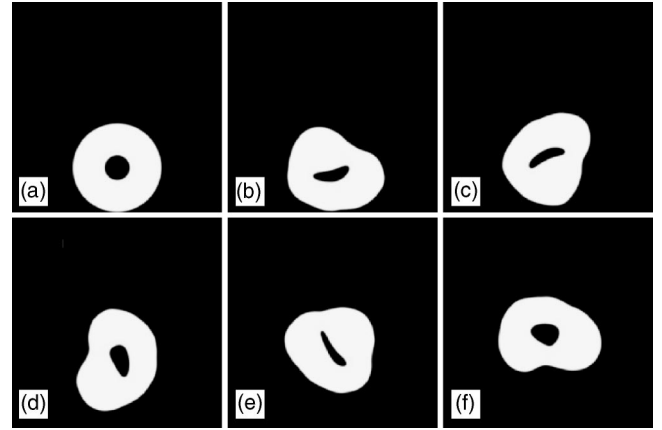


FIG. 4. Numerical simulation of the total reflection at a nonlinear-linear interface of a beam with a nested vortex of topological charge $l=4$ and a propagation constant $\beta=0.95\beta_{cr}$. The angle of incidence is $\alpha=0.25^\circ$. The propagation distances (in mm) are (a) $z=8$, (b) $z=88$, (c) $z=168$, (d) $z=248$, (e) $z=328$ and (f) $z=400$.

angular momentum. For higher values of l , this angle fluctuates around the value $\approx 0.25^\circ$.

We have performed a large series of numerical explorations for different angles of incidence α , ranging from quasi-elastic to the complete inelastic regime, showing that surface tension effect provides the beam a high stability. The simulations correspond to an initial radial stationary state calculated directly from the NLSE using a relaxation method. Our study covers a wide range of angular momentum or topological charge $l > 1$.

The typical beam widths used in the simulations are $\approx 20 \mu\text{m}$ for a given wavelength $\lambda=1.064 \mu\text{m}$ and a nonlinear phase shift of $n_2|\Psi|^2 \approx 0.01$. Numerical simulations are done with the standard split step Fourier transform method using FFTW algorithm on a 512×512 grid. The window width is $800 \mu\text{m}$.

A. Elastic regime: Small incidence angle

We shall first analyze the elastic regime, which corresponds to an incidence angle $\alpha < \alpha_{cr}$. As an example, in Fig. 4 we show the result of the numerical simulation of the total reflection at a nonlinear-linear interface of a beam with a nested vortex of topological charge $l=4$. The propagation constant is $\beta=0.95\beta_{cr}$ and the angle of incidence is $\alpha=0.25^\circ$ (which is below the critical angle α_{cr} , as can be appreciated in Fig. 3). In this case, the collision with the boundary produces a flattening of the initial beam when it impacts the boundary, so that the emerging beam preserves a compact support with the nested vortex of topological charge $l=4$.

Our computer simulations show that there is a deep analogy between incompressible fluid dynamics and the interference behavior at boundaries of the azimuthal beams studied previously. This can be understood by regarding vortex states as light condensates with a special type of surface tension — analogous to that of a liquid droplet— such that, above a critical value of the beam flux, is strong enough to retain the vortex without breaking.

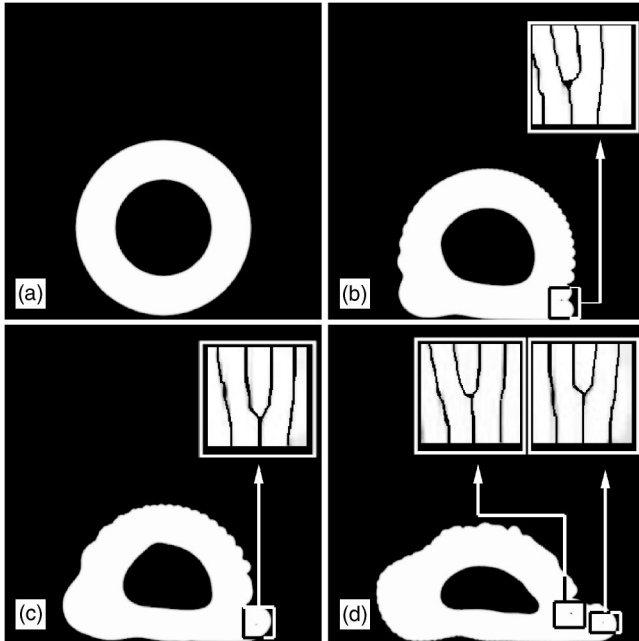


FIG. 5. Numerical simulation of the total reflection at a nonlinear-linear interface of a beam with a nested vortex of topological charge $l=9$ and a propagation constant $\beta=0.95\beta_{cr}$. The angle of incidence is $\alpha=1.0^\circ$. The propagation distances (in mm) are (a) $z=2$, (b) $z=18$, (c) $z=26$, and (d) $z=38$. The insets show the interference patterns with a slightly inclined plane wave.

B. Quasielastic regime: Vortex splitting without filamentation

Let us now consider the quasielastic regime, in which the angle of incidence is above its critical value α_{cr} . In order to show the effect of surface tension, we present three particular cases from our numerical investigation. All of them correspond to an initial radial stationary state of the propagation equation with $\beta=0.95\beta_{cr}$, and differ only in the topological charge l and the incidence angle α .

In Fig. 5, we show the result of the simulation of the total reflection of a beam with a nested vortex with topological charge $l=9$ and an incidence angle $\alpha=1.0^\circ$ at a planar boundary in a nonlinear-linear interface. In the insets we show the interference patterns with a slightly inclined plane wave. Note that the signature of a phase singularity is the fork defect in the fringe pattern where a new fringe starts at the location of the singularity. In this case, although the initial vortex of topological charge $l=9$ (a) does not disappear, we can see in (b) and (c) that a new small vortex of topological charge $l=1$ appears inside the compact support. In (d) we can distinguish two different vortices with angular momentum $l=1$.

The other case is shown in Fig. 6, where we have simulated internal reflection of a beam with a nested vortex with angular momentum $l=3$ inside a bulk cubic-quintic material surrounded by air. The angle of incidence is $\alpha=0.7^\circ$ (which is above the critical incidence angle α_{cr} , as can be seen in Fig. 3). The insets again show the interference patterns with a slightly inclined plane wave. As can be seen in the caption, the initial vortex (a) of topological charge $l=3$ is annihilated in (b) but the beam does not filament. This is due to surface

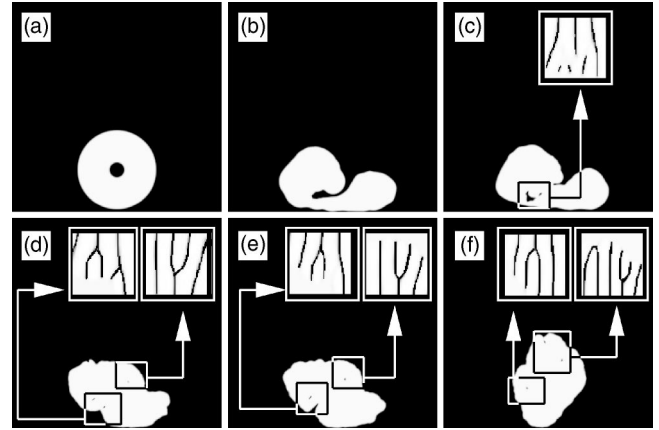


FIG. 6. Numerical simulation of the total reflection at a nonlinear-linear interface of a beam with a nested vortex of topological charge $l=3$ and a propagation constant $\beta=0.95\beta_{cr}$. The angle of incidence is $\alpha=0.7^\circ$. The propagation distances (in mm) are (a) $z=2$, (b) $z=52$, (c) $z=58$, (d) $z=70$, (e) $z=72$, and (f) $z=92$. The insets show the interference patterns with a slightly inclined plane wave.

tension that is strong enough to maintain the same average size. As can be seen in the caption, in (d) three small vortices with angular momentum $l=1$ appear inside the compact support. A curious fact is that in (e) one of these small vortices disappears but in (f) we can distinguish again three small vortices of angular momentum $l=1$.

The last case shown in Fig. 7 corresponds to the numerical simulation of the total reflection at a planar boundary of a beam with a nested vortex of angular momentum $l=6$. The angle of incidence is $\alpha=0.5^\circ$ (which is also above the critical incidence angle α_{cr} , as can be seen in Fig. 3). The top image shows the isosurface of the beam trajectory. The corresponding beam cross sections at different points are shown in the images (a)–(c). As can be appreciated, in this case the initial vortex state (a) suffers total reflection at the boundary between the nonlinear material and air (plane $y=0$), and then it splits into several vortices of lower topological charge l . In (c) we can see more clearly that the initial vortex of angular momentum $l=6$ has been annihilated and a new small vortex of topological charge $l=1$ has appeared, as it is shown in the interference pattern with a slightly inclined plane wave.

C. Inelastic regime: Vortex splitting with filamentation

We shall now study the complete inelastic regime, which corresponds to an incidence angle $\alpha \gg \alpha_{cr}$ that induces the breaking of the beam. As an example, we show in Fig. 8 the result of the numerical simulation of the total reflection of a beam with a nested vortex of topological charge $l=1$ and an incidence angle $\alpha=1.3^\circ$ at a planar boundary in a nonlinear-linear interface. The propagation constant is $\beta=0.95\beta_{cr}$. In the insets we show the interference patterns with a slightly inclined plane wave. As can be seen, in this case the initial vortex (a) suffers total reflection in (b), and in (c) the vortex has been annihilated. In (d) and (e) we can see how the compact support is strangulated. Finally, in (f), the beam fila-

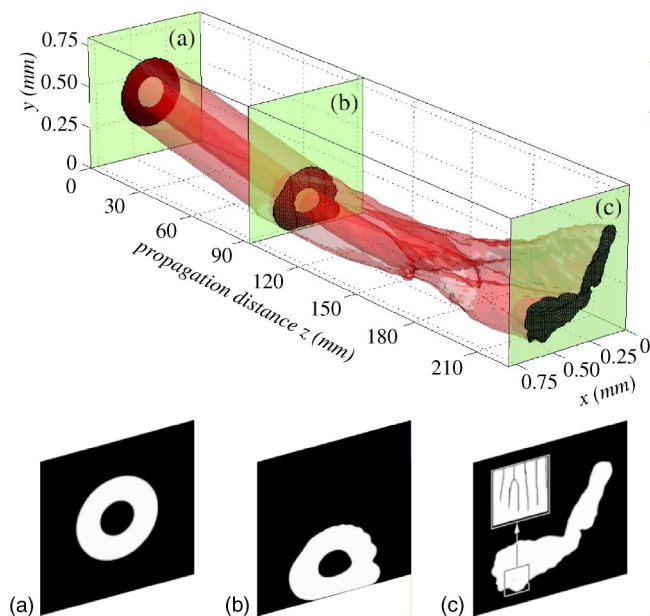


FIG. 7. (Color online) Numerical simulation of the total reflection at a planar boundary of a beam with a nested vortex of angular momentum $l=6$ and a propagation constant $\beta=0.95\beta_{cr}$. The angle of incidence is $\alpha=0.5^\circ$. The top image is the isosurface of the beam trajectory. The boundary between the nonlinear material and air is the plane $y=0$. The images (a)–(c) correspond to the beam cross section at different points. The inset in (c) shows the interference pattern with a slightly inclined plane wave.

ments because the surface tension is not strong enough to maintain the compact support without breaking.

V. CONCLUSIONS

We have analyzed the propagation of light beams with azimuthal vortices in cubic-quintic materials, showing that there is a deep analogy between total reflection at boundaries and the collision of a liquid droplet against a planar surface.

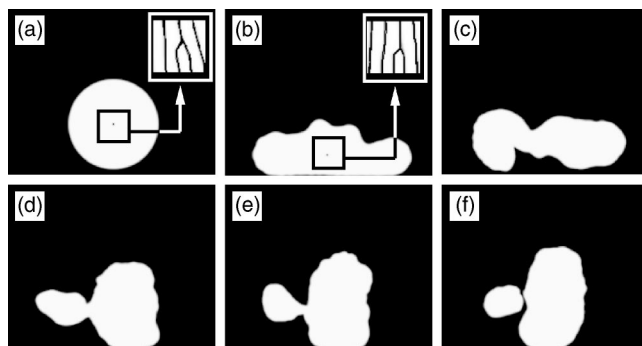


FIG. 8. Numerical simulation of the total reflection at a nonlinear-linear interface of a beam with a nested vortex of topological charge $l=1$ and a propagation constant $\beta=0.95\beta_{cr}$. The angle of incidence is $\alpha=1.3^\circ$. The propagation distances (in mm) are (a) $z=2$, (b) $z=22$, (c) $z=52$, (d) $z=66$, (e) $z=70$, and (f) $z=74$. The insets show the interference patterns with a slightly inclined plane wave.

We have performed a large series of numerical explorations for different angles of incidence and for different values of the angular momentum, from quasielastic to complete inelastic range. Our simulations show that the observed surface tension property provides the beam a high degree of stability, even if the hosted hole splits and decays to several vortices with lower values of l . In the limiting case of square beams, we have derived an expression for the surface tension of these light condensates, which grows linearly with the radius as in the case of usual liquid droplets. Our work adds extra support to the idea that light beams in cubic-quintic nonlinear materials can undergo a phase transition from a photon gas to a liquid of light. We have also calculated analytically the critical values of the propagation constant and the peak amplitude that characterize the domain existence of these vortices, which do not depend on the topological charge l .

ACKNOWLEDGMENT

This work was supported by CICYT Project No. TIC2000-1105-C03-01.

- [1] J. F. Nye and M. V. Berry, Proc. R. Soc. London, Ser. A **336**, 165 (1974).
- [2] L. Pismen, *Vortices in Nonlinear Fields* (Oxford University Press, London, 1999).
- [3] D. Rozas, Z. S. Sacks, and Jr. G. Swartzlander, Phys. Rev. Lett. **79**, 3399 (1997).
- [4] G. Indebetouw, J. Mod. Opt. **40**, 73 (1993).
- [5] N. R. Heckenberg, R. McDuff, C. P. Smith, and A. G. White, Opt. Lett. **17**, 221 (1992).
- [6] Yu. S. Kivshar and E. A. Ostrovskaya, Opt. Photonics News **12**, 24 (2001).
- [7] V. I. Kruglov and R. A. Vlasov, Phys. Lett. **111A**, 401 (1985).
- [8] Y. S. Kivshar, and B. Luther-Davies, Phys. Rep. **298**, 81 (1998).
- [9] V. Tikhonenko, J. Christou, and B. Luther-Davies, J. Opt. Soc. Am. B **12**, 2046 (1995).
- [10] W. J. Firth and D. V. Skryabin, Phys. Rev. Lett. **79**, 2450 (1997).
- [11] G. A. Swartzlander, Jr. and C. T. Law, Phys. Rev. Lett. **69**, 2503 (1992).
- [12] V. Tikhonenko and N. Akhmediev, Opt. Commun. **126**, 108 (1996).
- [13] M. Quiroga-Teixeiro and H. Michinel, J. Opt. Soc. Am. B **14**, 2004 (1997).
- [14] C. Josserand and S. Rica, Phys. Rev. Lett. **78**, 1215 (1997).
- [15] H. Michinel, J. Campo-Táboas, R. García-Fernández, J. R. Salgueiro, and M. L. Quiroga-Teixeiro, Phys. Rev. E **65**, 066604-1-7. (2002).
- [16] H. Michinel, J. Campo-Táboas, M. L. Quiroga-Teixeiro, J. R. Salgueiro, and R. García-Fernández, J. Opt. B: Quantum Semi-classical Opt. **3**, 314 (2001).
- [17] D. E. Edmundson and R. H. Enns, Phys. Rev. A **51**, 2491

- (1995).
- [18] F. Smektala, C. Quemard, V. Couderc, and A. Barthelemy, *J. Non-Cryst. Solids* **274**, 232 (2000).
- [19] A. H. Piekara, J. S. Moore, and M. S. Feld, *Phys. Rev. A* **9**, 1403 (1974).
- [20] K. Dimitrievski, E. Reimhult, E. Svensson, A. Öhgren, D. Anderson, A. Berntson, M. Lisak, and M. L. Quiroga-Teixeiro, *Phys. Lett. A* **248**, 369 (1998).
- [21] M. L. Quiroga-Teixeiro, A. Berntson, and H. Michinel, *J. Opt. Soc. Am. B* **16**, 1697 (1999).